Research on Ultrasonic Calibration Method of Contacting surface Pressure Based on Fillet Plane Contact

Jiecheng Ding[1] , Bo Yuan[1] , Xiaodong Li[1] ,Cong Yue[2] , Qingkai Han[1] , Wei Sun[1]*

1.School of Mechanical Engineering, Dalian University of Technology, Dalian, Liaoning 116023
2.AECC Commercial aircraft engine CO.,LTD, Shanghai 201109

Abstract: In order to realize the pressure distribution of the bolt contacting surface, it is necessary to establish an ultrasonic reflectivity - pressure relationship curve. By detecting reflectance of the ultrasonic wave at the binding surface, the plane contact theory on the basis of the fillet, the pressure distribution status was derived, and compared with the results of the finite element, to verify the correctness and viability. At the same time, it is fitted with the ultrasonic reflectivity distribution detected by the ultrasonic transducer, and then a certain calibration method is used to construct the ultrasonic calibration curve. Calibration curve is consistent with the existing conclusion, indicating that the ultrasound calibration method can be applied to the actual calibration process.

Keywords: Rounded plane contact theory; Calibration curve; Contacting surface; Pressure distribution

1 Introduction

"Made in China 2025 " puts higher demands on Chinese manufacturing. For high-end mechanical equipment, mechanical joint performance has a crucial impact on overall machine performance , such as static and dynamic characteristics, vibration resistance, and rapid response to motion . The contact pressure and stiffness distribution of the contacting surface are important parameters for measuring the assembly quality. To study the performance characteristics of the machine, it is necessary to accurately detect the contacting surface performance . Due to the disorder, randomness and multi-scale of the machined surface, complex and microscopic elastoplastic deformation occurs when the contacting surface is stressed, so the contact characteristics of the contacting surface have obvious nonlinear characteristics [1] . [1]

In terms of the theory of combined surface contact states , Greenwood et al[2] assumed that the microscopic contour height of the rough surface obeys the Gaussian distribution and proposes a G- W contact model. Whitehouse et al[3] explored the

*Corresponding author (sunwei@dlut.edu.cn)
ISSN 2572-4975 (Print), 2572-4991 (Online)

properties of curvature correlation in the peak height and peak top of the probability density function, and proposed the WA model. Srinivasan et al[4] proposed surface feature representation based on fractal theory and including contour structure features. Huihong Dang[5] calculated the distribution of surface micro protrusion based on fractal theory, and gave a mathematical model of the normal contact stiffness of the contacting surface. Runqiong Wang[6] introduced the micro-contact cross-sectional area distribution function based on fractal geometry theory and domain expansion factor, and gave a contacting surface contact stiffness fractal model considering the influence of surface micro-convex interaction. In the ultrasonic contacting surface state testing, scholars also a lot of research work, Massimiliano[7] [8] used ultrasonic to detect the pressure distribution of the bolt contacting surface and the contacting surface of the train wheel and the track, and compared it with the Hertz contact theory. J Zhao et al[9] gave a new signal processing technique in ultrasonic testing to improve lateral resolution and detection accuracy. Bickford et al [10] proposed the use of hollow cylinders, spheres and cones to simplify the contact area of the joint, which allows the state of the connected parts to be mathematically analyzed. Fei Du et al[11] proposed a new deconvolution method to accurately estimate the noise of the experimentally extracted reflection matrix for the influence of the fuzzy effect of the ultrasonic probe focus on the detection accuracy. In the aspect of ultrasonic contacting surface calibration , Fei Du et al [12] used the mean reflectance of the scanning points in the flat region of the joint pressure center and the corresponding pressure fitting to obtain the initial pressure - reflectance relationship.Weixin Tang et al[13] based on the simple spring model experimental protocol designed for measuring two steel blocks binding portion of the contact stiffness with ultrasonic waves, the ultrasonic pressure to give the corresponding relationship by the pressure signal amplitude averaging method. AMQuinn et al[14] using the ultrasonic measuring a contact pressure between the two elements, and using the numerical model of the contact fitting the relationship between the pressure and the ultrasonic reflectivity.

In the present study, although the state has established contact with a lot of theory, but the theory does not correspond to the way up and calibration, in establishing the relationship between pressure and ultrasound reflectivity, commonly used pressure averaged way, but the actual pressure distribution will As the structure changes, the pressure distribution is uneven, which causes the original method calibration results to have errors . Aiming at this problem, this paper applies the theory of fillet plane contact to ultrasonic calibration method , deduces the contact problem considering the fillet, and verifies it by finite element method, and establishes the relationship between ultrasonic reflectivity and pressure by experiment. Compared with the existing literature, the feasibility of the method is further verified, which lays a foundation for the detection of the actual contacting surface.

 ISSN 2572-4975 (Print), 2572-4991 (Online)

2 Theoretical calculation of pressure distribution calculation

M. Ciavarella[15] [16] studied the plane upon contact with, pyramid indenter geometry affect the shape of the head and the platen different loading situations. The theoretical model is shown in Fig.1.

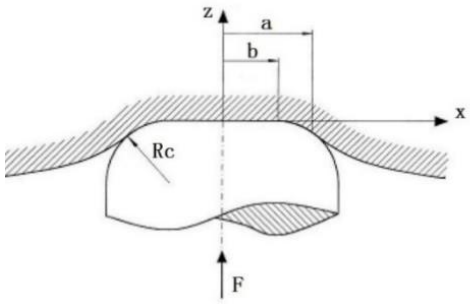

Fig.1. Rounded plane contact theoretical model diagram

Where R c represents the fillet radius, b is the radius of the circle, a is the actual contact radius, and F is the applied force.

In the case of the large fillet planar contact plane, so long as the contact plate does not enter the chamfered regions, namely: the figure below, a is not close to the b + Rc, there is sufficient material around the contact therewith, provide a biasing force.

In the case of normal normal contact, the pressure distribution p(r) and the contact area S can represent the surface normal displacement $u_z(r)$

$$u_z(r) = \frac{A}{2\pi}\iint \frac{p(r')}{R} dS, 0 \le r \le a \tag{1}$$

among them, r′ is the radial coordinate of the integration point, A is the characteristic parameter of the material, and the specific definition is as follows:

$$\frac{A}{2} = \frac{1-v_1^2}{E_1} + \frac{1-v_2^2}{E_2} \tag{2}$$

among them E_i is Young's modulus, V_i is Poisson's ratio.

At different radii, the following relationship exists between the surface normal displacement $u_z(r)$ and the contour radius z(r) :

$$\begin{cases} u_z(r) = \alpha_n - z(r), 0 \le r \le a \\ u_z(r) > \alpha_n - z(r), a \le r \end{cases} \tag{3}$$

Where $u_z(r)$ is the surface normal displacement and z(r) is the contour radius,α_n is the distance between two remote points in the contact area.

Based on the above relationship, based on the actual basic situation, the relationship between the following pressure distributions is obtained.

$$p(r) = -\frac{2}{\pi A}\int_r^a \frac{F(s)ds}{\sqrt{s^2 - r^2}}, 0 \le r \le a \tag{4}$$

Subsequently, the concept of α_n model angle is introduced, and the contact theory formula was further proposed.

$$\frac{p(r)}{p_m}=\frac{3\cos\varphi_0}{3\sin\varphi_0+\sin^3\varphi_0-3\varphi_0\cos\varphi_0}\psi_f\left(\frac{r}{b}\right),0\le r\le a \tag{5}$$

$$\psi_f(x)=\begin{cases}\int_0^{\varphi_1}\frac{(2\tan\varphi-\varphi)\tan\varphi d\varphi}{\sqrt{1-x^2\cos^2\varphi}}, & 0<x<1\\ \int_{\arccos\left(\frac{1}{x}\right)}^{\varphi_1}\frac{(2\tan\varphi-\varphi)\tan\varphi d\varphi}{\sqrt{1-x^2\cos^2\varphi}}, & 1<x\le\frac{1}{\cos\varphi_0}\end{cases} \tag{6}$$

Finally, the above two formulas, derived rounded planar contact theory this system adopts the formula:

$$p(r)=\frac{2k}{\pi A}\begin{cases}\int_b^a\frac{\left(2\sqrt{s^2-b^2}-b\times\arccos\frac{b}{s}\right)ds}{\sqrt{s^2-r^2}}, & 0<r<b\\ \int_r^a\frac{\left(2\sqrt{s^2-b^2}-b\times\arccos\frac{b}{s}\right)ds}{\sqrt{s^2-r^2}}, & b<r<a\end{cases} \tag{7}$$

Among them, $k=\frac{1}{R_c}$, $A=2\left(\frac{1-V_1^2}{E_1}+\frac{1-V_2^2}{E_2}\right)$, V_i is the Poisson's ratio of the material, E_i is the Young's modulus of the material, a is the average boundary eigenvalue, Rc is the fillet radius of the fillet plane of the fillet plane, b is the plane radius of the fillet plane, and s is the characteristic variable .

3 Comparison and analysis of finite elements

3.1 Finite element model

To verify the validity of the theory of planar contact fillet derived using finite element software COMSOL simulation analysis. According to the actual situation, the material of the model is steel. The elastic modulus is 2.1×10^5Mpa and the Poisson's ratio is 0.30. The boundary condition is: applying a fixed constraint to the upper edge of the upper test piece, and applying a specified displacement to the lower edge of the lower test piece to contact. Then apply a load to ensure the convergence of the calculation. At the same time, the entire model adopts axisymmetric constraints to simplify the calculation process.

ISSN 2572-4975 (Print), 2572-4991 (Online)

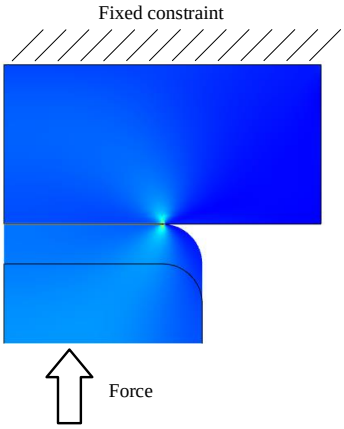

Fig.2. Finite element analysis model

3.2 Simulation analysis result

When the loaded force changes from 1t,2t,and 3t,the results of the finite element analysis are compared with the derived rounded contact theory. The following is a comparison of the relationship curves of the two methods. It can be seen from the three comparison graphs that the theoretical value is slightly lower than the simulated value of the finite element to a certain extent,but is similar in general trend. Moreover, the diffience between the relationship curve obtained by the finite element and the theory is not very large. Therefore, it is further proved that the derived rounded plane contact theory is correct and feasible, and the theoretical basis for the subsequent detection.

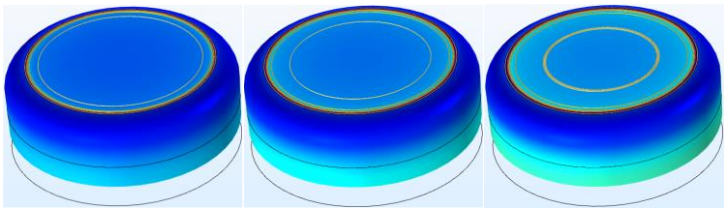

(a) (b) (c)

Fig.3. Finite element result graph
(a) loaded force is 1t (b) loaded force is 2t (c) loaded force is 3t

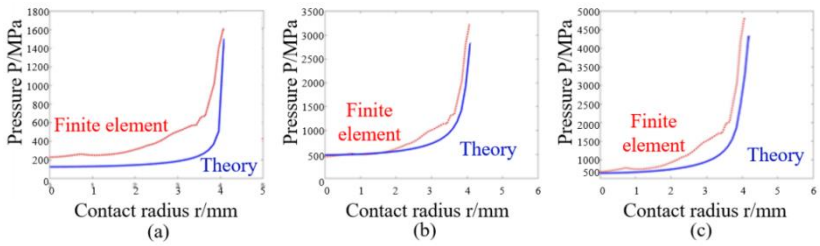

Fig.4. Comparison of finite element and theoretical value (a) loaded force is 1t (b) loaded force is 2t (c) loaded force is 3t

4 Establishment of ultrasonic calibration curve

4.1 Experimental device and test piece

The same contact model is used to illustrate the method of establishing the ultrasonic calibration curve. As shown in Fig. 5 , loading of the contacting surface is achieved by using a loading device.Ultrasonic pulse signals are transmitted and received using a 5MHz water immersion focused ultrasound probe, 5700 PR ultrasonic pulsed receiver. The Tektronix TDS3012C oscilloscope is used to acquire signals from the ultrasonic pulse-transmitting receiver, while the data is stored and analyzed on the PC side using Labview (communication via the GPIB line). The hydraulic jack is used to load the contacting surface, and the pressure sensor performs pressure collection.

In the experiment, the upper test piece has a diameter of 8 mm and a height of 3 mm . The lower test piece is a combination of a cylinder having a diameter of 5 mm , a height of 3 mm and a rounded corner of 2 mm . The materials are all 45 steel, the surface roughness of the contact surface is 0.8μm.

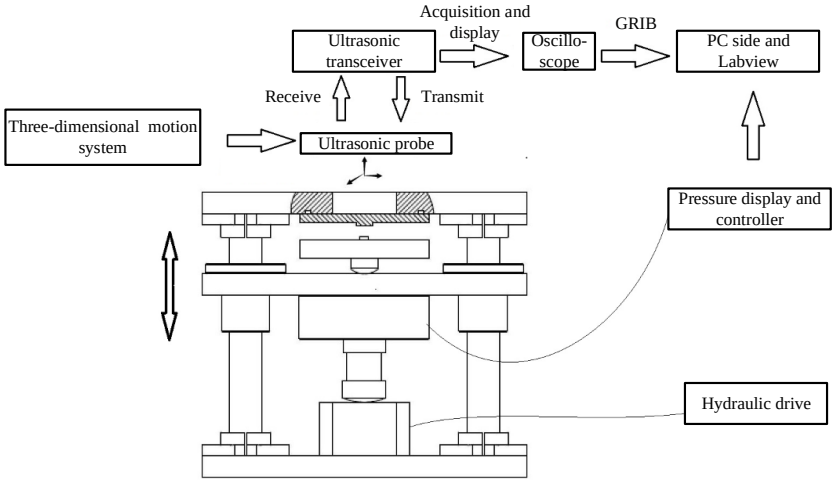

Fig.5. Calibration process schematic

4.2 Calibration curve establishment process

In order to construct a calibration curve for ultrasound, it is necessary to establish the relationship between reflectance and contact radius$R=f_1(r)$, and the relationship between pressure and contact radius $P=f_2(r)$.Then, the variable r is eliminated. The obtained relationship curve is processed by a certain error elimination method to obtain the final ultrasonic calibration curve.

The test piece material of the calibration process was 45 steel, and the surface roughness was 0.8 μm. The center of the lower test piece is designed with a small cylindrical boss of 10 mm in diameter, which is in contact with the large cylindrical boss of the upper test piece having a diameter of 16 mm. The upper test piece is

 ISSN 2572-4975 (Print), 2572-4991 (Online)

connected to the upper panel through the external thread, and a sealing ring is arranged in the middle thereof to adapt to the detection condition of the water immersion probe when the water is used as a coupling agent.

Table 1. Test condition table

Parameter	Value
Empty travel speed	10 mm/s
Detection speed	1mm/s
Detection interval	0.1mm/s
Detection distance	10.37mm
Loading travel itinerary	24mm
Loading range	24mm

1) Determine the center position: Firstly , the position of the system is determined by using the three-dimensional mobile platform , and the center position of the test piece is obtained by laser detection to be O_1 (x_0 ,y_0).

2) Get zero signal: in the absence of loading conditions, using V312-0.25-5MHz-PTF ultrasonic transducer reference center position of the specimen, a "serpentine" manner, intervals of 0.1mm, a height of 10.3 mm detect C- scan is performed, and its signal is used as a zero point signal for the reflectance .

3) Acquire the characteristic signal: keep the upper test piece not moving, and let the upper and lower test pieces touch. Under the three loads of 1t, 2t, and 3t , the C-scan is performed with the same trajectory using the ultrasonic transducer , and the signal is used as a characteristic signal for the reflectance.

4) Extraction and the calculated reflectivity characteristic boundary value: Fast Fourier Transform (FFT) for zero and characteristic signals, while utilizing the following equation, to calculate the corresponding ultrasonic wave reflectivity; while taking advantage of the distribution of reflectance , the boundary feature value a i is determined, and the average boundary feature value a is calculated.

$$R = \frac{h_i}{H_i} \tag{8}$$

R is the reflectivity of the ultrasonic wave, h_i is the magnitude of the characteristic signal, H_i is the amplitude of the zero signal, R_i is the reflectivity for different loads .

Using the derived formula and the previously determined boundary feature value a, the distribution curve of the pressure under the corresponding load is calculated.

$$p(r) = \frac{2k}{\pi A}\begin{cases} \int_b^a \frac{\left(2\sqrt{s^2-b^2} - \operatorname{barccos}\frac{b}{s}\right) ds}{\sqrt{s^2-r^2}}, 0 < r < b, \\ \int_r^a \frac{\left(2\sqrt{s^2-b^2} - \operatorname{barccos}\frac{b}{s}\right) ds}{\sqrt{s^2-r^2}}, b < r < a \end{cases} \tag{9}$$

k = $\frac{1}{R_c}$, A= $2(\frac{1-V_1^2}{E_1} + \frac{1-V_2^2}{E_2})$(Vi is the Poisson's ratio of the material, Ei is the Young's modulus of the material) , a is the boundary feature value, and the plane radius of the b contact.

Calculate the theoretical pressure distribution by using the initial reflectance - pressure relationship curve of the ultrasonic reflectance distribution under different loads previously detected , and calculate the total load W_i' by means of integration, divide the actual load W_i measured by the pressure sensor using the calculated total load W_i', get correction factor K_i.Finally, take the average value K.

$$W_i' = \int P_i' dxdy \tag{10}$$

$$K_i = \frac{W_i}{W_i'} \tag{11}$$

W_i' is the calculated total load, P_i' is the calculated pressure, K_i is the correction factor, W_i is the actual load. The initial reflectance-pressure relationship curve is corrected by the average correction coefficient K to obtain the final reflectance-pressure relationship curve.

$$P_i = K_i \times P_i' \tag{12}$$

Under the three conditions of loading, 1t, 2t, and 3t, the ultrasonic reflectance distribution and its corresponding pressure distribution obtained by the system scanning are shown in Fig 6:

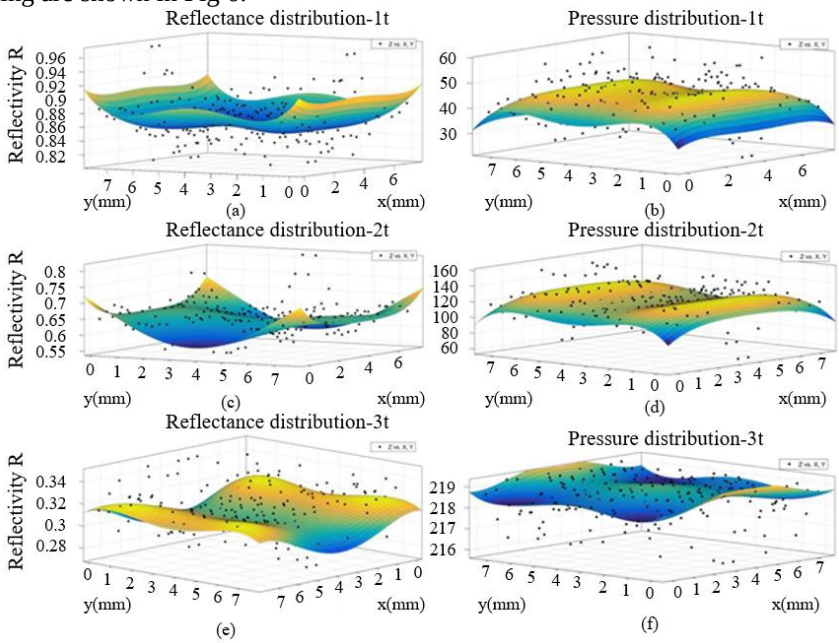

Fig.6. Ultrasonic reflectivity and pressure distribution

4.3 Comparison of results

In this paper, the method based on the theory of rounded plane contact is used to complete the construction of the ultrasonic calibration curve, and the comparison with the relevant literature is carried out. The method of this paper considers the pressure distribution of the contact contacting surface, rather than a single method of using the

ISSN 2572-4975 (Print), 2572-4991 (Online)

average pressure to carry out data processing, and there will be some improvement in the accuracy of the results.

Fig 7 uses the Gaussian function to fit the experimental data. Using Matlab to fit the curve, the final ultrasonic reflectance - pressure relationship curve is expressed as follows:

$$R = 9.41 \times 10^{20} \times e^{-\left(\frac{P+2.089\times10^4}{2998}\right)^2} \quad (13)$$

R is the ultrasonic reflectivity and P is the pressure at the contacting surface.

The comparison results show that after using the rounded plane contact theory and a certain error elimination method, the obtained relationship curve is basically the same as other literatures [11].

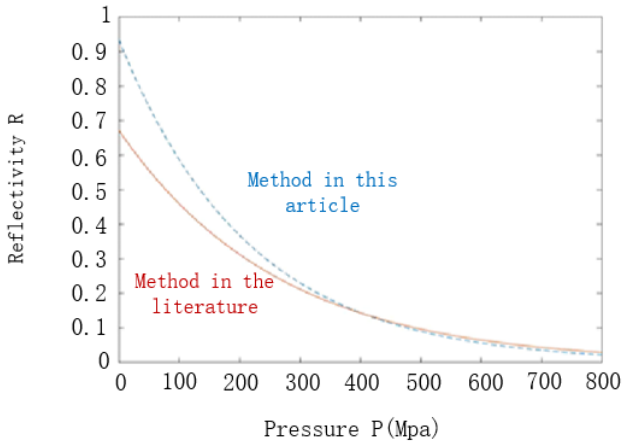

Fig.7. Ultrasonic reflectance-pressure curve

5 Conclusions and discussion

In this paper, a method of ultrasonic calibration combined with surface pressure considering the distribution of surface pressure is proposed. On the basis of further deriving the theory of fillet plane contact , the method of ultrasonic calibration curve was studied. The results are as follows:

(1) through the finite element model, and the results with theoretical results radiused planar contact contrast, the validity of the theory of planar contact radiused deduced.

(2) The calibration process considers the pressure distribution of the contacting surface, and improves the accuracy of the calibration curve compared with the pressure averaging method. At the same time, iterative elimination is used to further eliminate the influence of other factors on the calibration results .

(3) The calibration results of the method show that the reflectivity of the ultrasonic wave decreases with the increase of the pressure of the contacting surface.

Compared with the related literature, the calibration results are roughly the same, which verifies the effectiveness of the method described in this paper.

In the future , the ultrasonic reflectivity-pressure curve obtained by the method can be applied to the detection of actual equipment.

Acknowledgement

This work is supported by the Major special basic research projects(No. 2017-VII-0010-0105), Shanghai Sailing Program(No.19YF1452400) and the Fundamental Research Funds for the Central Universities of China (No.DUT18LAB04).

References

1. X. Huang. Study on bolt connection stiffness considering joint contact. Dalian University of Technology,2016.
2. Greenwood, James A , and J. B. P. Williamson . "The contact of nominally-flat surfaces." ***Proceedings of the Royal Society*** **29**5(1966).
3. Whitehouse, D. J. , J. F. Archard . "The Properties of Random Surfaces of Significance in their Contact." ***Proceedings of the Royal Society A: Mathematical, Physical and Engineering Sciences*** 316.1524(1970):97-121.
4. Srinivasan, R. S. , K. L. Wood . "A Form Tolerancing Theory Using Fractals and Wavelets." ***Journal of Mechanical Design*** 119.2(1997):185.
5. Srinivasan, R. S. , Wood, K. L. . (1997). A form tolerancing theory using fractals and wavelets. ***Journal of Mechanical Design***, 119(2), 185.
6. R.Q. Wang, L.D. Zhu，C.X. Zhu. Fractal model of contacting surface contact stiffness based on surface micro-convex interaction effects. ***Journal of Mechanical Engineering.***
7. Pau M, Baldi A. Application of an Ultrasonic Technique to Assess Contact Performance of Bolted Joints. ***Journal of Pressure Vessel Technology***, 2007, 129(1): 175-185.
8. Pau, Massimiliano , B. Leban , A. Baldi . "Simultaneous subsurface defect detection and contact parameter assessment in a wheel–rail system." ***Wear*** 265.11-12(2008):1837-1847.
9. Zhao, J. , P. A. Gaydecki , F. M. Burdekin . "Investigation of block filtering and deconvolution for the improvement of lateral resolution and flaw sizing accuracy in ultrasonic testing." ***Ultrasonics*** 33.3(1995):187-194.
10. BICKFORD J. Introduction to the Design and Behavior of Bolted Joints, Fourth Edition: Non-Gasketed Joints . ***Crc Press***, 2007.
11. F. Du, J. Hong, B.T. Li, et al. Study on Ultrasonic Testing Method of Contacting surface Parameters. ***Journal of Xi'an Jiaotong University***, 2013,47 (3): 18-23.
12. B.T. Li, F. Du , J.H. , et al . Construction method of pressure - ultrasonic reflectance curve for contacting surface pressure detection.
13. W.X. Tang, Q. Yin, X.F. ZHAO, G.F. Yin, Y. Zhao, M. Li. Mechanical contacting surface. ***Chinese contacting ultrasonic testing method for testing stiffness***, 2015,41 (08): 8-12.
14. Quinn, A. M , B. W. Drinkwater , R. S. Dwyerjoyce . "The measurement of contact pressure in machine elements using ultrasound." ***Ultrasonics*** 39.7(2002):495-502.

 ISSN 2572-4975 (Print), 2572-4991 (Online)

15. Ciavarella, M. "Tangential Loading of General Three-Dimensional Contacts." ***Journal of Applied Mechanics*** 65.4(1998):998.
16. CIAVARELLA MHDA M. The influence of rounded edges on indentation by a flat punch. ***Proceedings of the Institution of Mechanical Engineers, Part C: Journal of Mechanical Engineering Science***, 1998, 212(4): 319-327.